JOURNAL OF MATERIALS SCIENCE 24 (1989) 3497–3503

High temperature studies of Fe–Mn–Al–C alloys with different manganese concentrations in air and nitrogen

W. S. YANG, C. M. WAN
Department of Materials Science and Engineering, National Tsing Hua University, Hsinchu, Taiwan, 30043

The formation of AlN was studied using a series of Fe–Mn–Al–C alloys with manganese contents from 20 to 40 wt%. All investigations were carried out in air and nitrogen at 1000° C. The permeability ($D_N N_N$) of nitrogen in Fe–Mn–Al–C alloys was found to be a major factor influencing the formation of AlN precipitates which are always observed underneath the oxide scales of the specimen. The formation of AlN is related to the lower formation rate of Al_2O_3 and high permeability of nitrogen; therefore AlN can only be formed in those alloys with a higher manganese concentration because the specimens are treated in air and in pure nitrogen at 1000 C.

1. Introduction

Alloys which are designed for applications in high temperatures need both high-temperature strength and high-temperature corrosion resistance. In general, alloys with an austenite phase have a better strength at high temperature and better toughness at low temperature than those alloys with a ferrite phase. In the Fe–Al alloy system, as the aluminium content exceeds 7 wt%, it is well known that Fe–Al alloy will have excellent high-temperature oxidation resistance due to the formation of a protective Al_2O_3 layer. However, Fe–Al alloys are always very brittle [1] even at room temperature and have a poor high-temperature strength and poor machinability. The involvement of manganese and carbon can stabilize Fe–Al alloys at a full austenite phase [2, 3]. In general, this causes the alloys to shift to another alloy system, i.e. the Fe–Mn–Al–C based alloys.

In past years, most studies on the high-temperature resistance of Fe–Mn–Al–C alloys have been concentrated on the oxides and their formation in air and oxygen [2–5]. However, there are few specific studies of nitrogen as a second oxidant for the Fe–Mn–Al–C alloy, even though the high-temperature oxidation studies are carried in air. Fe–Mn–Al–C alloys always have a very high aluminium concentration, therefore it is unreasonable to neglect the influence of nitrogen, because the high-temperature experiment is performed in a gas with high nitrogen content at 1000° C, such as air. This is due to the fact that AlN is easily formed at high temperatures. For the past few decades, much research work has been carried out on the oxidation of Fe–Mn–Al based alloy in air. But the existence of AlN was not pointed out and proved by X-ray diffraction technique until 1986 [6]. The most possible reason may be that AlN is so easily confused with aluminium oxides. In the observations of Lopes and Assuncao [6], many aluminium-rich needle- or plate-like structures are found underneath the oxide scales. The plate-like structure will consume the aluminium in the matrix and becomes some kind of easy diffusion path for oxygen, nitrogen, manganese, and others. Obviously, it would then play an important role in high-temperature oxidation and corrosion resistance [7]. Recently, the needle- or plate-like structure have again been identified by TEM SADP technique to be AlN [7].

According to Lopes and Assuncao's report [6], Fe–36.47Mn–7.38Al–0.13C develops AlN structure at 1000° C in air. On the other hand, it is quite interesting that no AlN can be observed in Fe–Al–C [8] and Fe–Al [9] alloys, as oxidation is again carried out in air. A former report [7] indicates that the degree of solubility of nitrogen in Fe–Mn–Al–Cr–C alloy plays a major role in the AlN nitride formation for the alloy. Manganese is well known to render a high solubility of nitrogen in the alloy, especially in steel with austenite structure. Therefore, it is quite reasonable that no AlN is found in Fe–Al–C and Fe–Al alloys, where high-temperature experiments are carried out in air as the solubility of the nitrogen in the alloys is still very low. The present work concentrates on the effects of different manganese contents (20 to 40 wt%) in a series of Fe–Mn–Al–C alloys on the high-temperature behaviour in both nitrogen and air at 1000° C.

2. Experimental procedure

Five Fe–Mn–Al–C alloys with different manganese contents were used in this study and their chemical compositions are listed in Table I.

The alloys were prepared from pure iron, electrolytic manganese and high-purity aluminium by an air induction melting furnace. The cast ingots were first homogenized at 1100° C for 4 h and hot forged at 1200° C with 50% reduction. Then the second

0022–2461/89 $03.00 + .12

homogenization at 1100° C for 1 h followed. After surface finishing, the cold-rolled plates were solution treated at 1050° C with argon protection. Two different sizes of specimens for each alloy were prepared for the present study. Specimens with dimension 2 mm × 15 mm × 20 mm were prepared for X-ray diffraction investigation and oxide morphology studies, the other specimens for kinetics studies, had dimension of 2 mm × 4 mm × 8 mm. Before the high-temperature experiment, all the specimens were mechanically polished with abrasive paper up to 1200 grit and cleaned ultrasonically in acetone. The present high-temperature studies were carried in high-purity nitrogen gas (99.9995%), and dry air under static conditions at 1000° C. Kinetics measurements were carried using an infrared image furnace combined with an ULVAC/SHRINK-URZKO thermobalance. The heating and cooling rate of the infrared image furnace was 100° C min^{-1}. High-temperature experiments for the specimens which are prepared for X-ray diffraction and metallography observation were performed in an atmosphere-control tube furnace. After high-temperature experiments at 1000° C were completed, all the specimens were removed rapidly and air-cooled.

The possible phases formed on the surface of the specimen after the high-temperature experiment were identified using a Rikagu X-ray diffractometer. The morphologies of the oxide layer were examined by both optical microscopy and scanning electron microscopy. The elemental distributions for the oxide scale were also investigated by using the X-ray mapping technique.

3. Results

3.1. Characteristics of alloys before high-temperature experiment

In addition to the optical metallography investigation, X-ray diffraction techniques are also performed on the alloys after 1050° C solution treatment. All the alloys are determined to be fully austenite and are shown in Fig. 1; therefore, this reveals that all the present alloys are fully austenite before the high-temperature experiment.

TABLE I

Alloy	Mn (wt %)	Al (wt %)	C (wt %)	Fe (wt %)
A	20.5	7.15	0.876	Bal.
B	26.4	7.00	0.860	Bal.
C	30.9	7.42	0.880	Bal.
D	37.4	7.12	0.900	Bal.
E	41.5	7.14	0.935	Bal.

3.2. Behaviour in nitrogen

As the experiments were carried out in nitrogen for all the alloys used here at 1000° C, many needle-like particles were always observed along the alloy/matrix interface. Figs 2a to e show the microstructure of all the alloys after the high-temperature experiment in nitrogen at 1000° C for 12 h, indicating that the depth of the layer which contains the needle-like structure increases with increasing manganese content in these alloys. X-ray mapping of the needle-like structure for alloy E is shown in Fig. 3. It may be seen that the needle-like structure is rich in aluminium and poor in iron and manganese. Combined with the X-ray diffraction pattern as shown in Fig. 4, the needle-like structure is identified as AlN.

The kinetic curves from the high-temperature experiment in pure nitrogen at 1000° C always give a confusing result, because the influence of oxygen is very difficult to avoid in the hot stage of a thermobalance. Therefore, kinetics studies of the alloys used in nitrogen are neglected.

3.3. Behaviour in air

Kinetics measurements for the present alloys used in the high-temperature experiment in air at 1000° C are shown in Fig. 5. The kinetics results indicate that increasing the manganese content in the present work is detrimental to the oxidation resistance in air at 1000° C. The morphology of the oxide layer for alloy A after 6 h at 1000° C in air is shown in Fig. 6. The gap between the external oxide layer and the internal oxide layer is believed to be introduced by the cooling process after the alloy is removed from the furnace. From X-ray diffraction determination and X-ray mapping

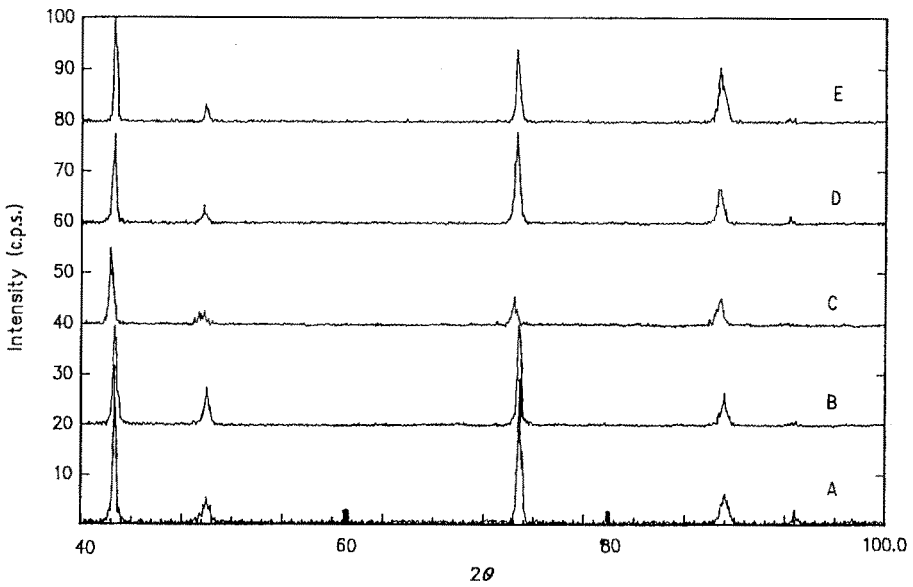

Figure 1 X-ray diffraction patterns of the alloys used before high-temperature treatment.

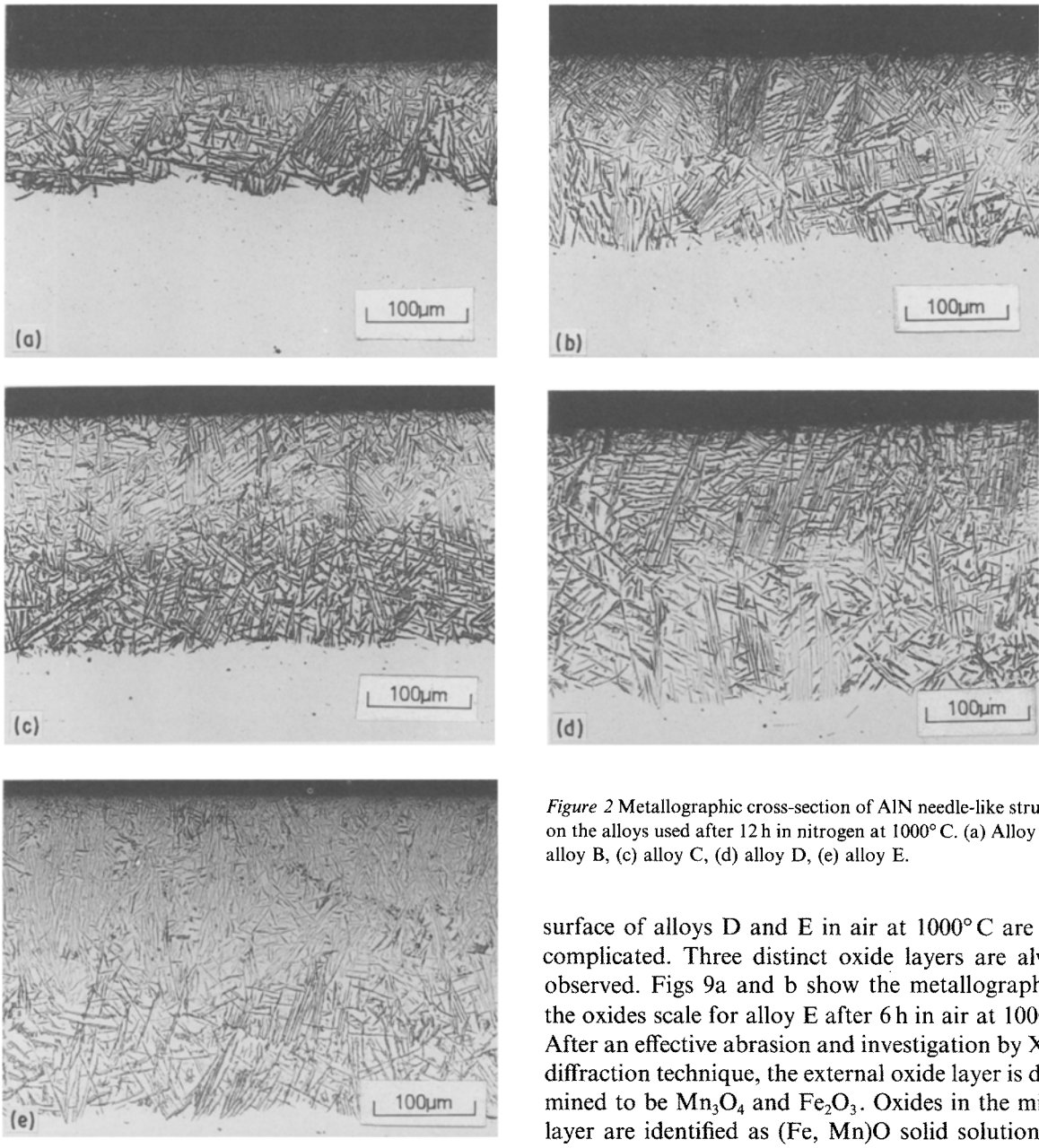

Figure 2 Metallographic cross-section of AlN needle-like structures on the alloys used after 12 h in nitrogen at 1000° C. (a) Alloy A, (b) alloy B, (c) alloy C, (d) alloy D, (e) alloy E.

(Fig. 7), the oxides formed on the surface of alloy A are identified as (Fe, Mn)$_3$O$_4$, Fe$_2$O$_3$, and (Fe, Mn)Al$_2$O$_4$. Here, the (Fe, Mn)Al$_2$O$_4$ spinel is always observed along the oxide/alloy interface. After the 1000° C treatment in air, the external oxides of alloy B are easily spalled off during the cooling process. Therefore, these oxides must be carefully collected and ground to powder for X-ray analysis. From the mixed powder, the spalled oxides are identified as Mn$_3$O$_4$ and some Fe$_2$O$_3$. In addition, a grey lamellar structure in the inner oxide matrix is always observed. X-ray mapping of the inner oxide matrix is shown in Fig. 8, which indicates the lamellar phase to be rich in aluminium. Combination of the elemental distribution and the X-ray diffraction pattern indicates that the grey lamellar phase may be concerned with the mixing of (Fe, Mn)Al$_2$O$_4$ spinel and the (Fe, Mn)$_3$O$_4$ solid solution. The formation of lamellar (Fe, Mn)Al$_2$O$_4$ is possibly concerned with the breaking away and healing mechanism. The oxide scales which are formed on the surface of alloys D and E in air at 1000° C are very complicated. Three distinct oxide layers are always observed. Figs 9a and b show the metallography of the oxides scale for alloy E after 6 h in air at 1000° C. After an effective abrasion and investigation by X-ray diffraction technique, the external oxide layer is determined to be Mn$_3$O$_4$ and Fe$_2$O$_3$. Oxides in the middle layer are identified as (Fe, Mn)O solid solution and (Fe, Mn)Al$_2$O$_4$ spinel, and the inner portion contains many AlN particles. In the present work, it is interesting to find that AlN is always observed in alloys in which the manganese content is over 30 wt % and the aluminium content is about 7 to 7.5 wt %.

4. Discussion

4.1. Behaviour in nitrogen

The standard Gibbs free energy for the formation of AlN is $-44.7\,\text{kcal mol}^{-1}$ at 1000° C [11]. In the present work, no precipitate and ordering can be observed in all the alloys A, B, C, D, E. Therefore, it is reasonable to assume that the alloys used obey the ideal solution behaviour. The Gibbs free energy for formation of AlN can be calculated to be about -39.54 and $-39.26\,\text{kcal mol}^{-1}$ for the alloy used in nitrogen and air at 1000° C, respectively. In addition, AlN precipitates are always observed in all the present alloys after the 1000° C treatment in nitrogen. This reveals that nitrogen can always react with aluminium in these alloys at 1000° C in a nitrogen atmosphere. The internal nitridation in the present work is thought to be concerned with the process where the nitrogen

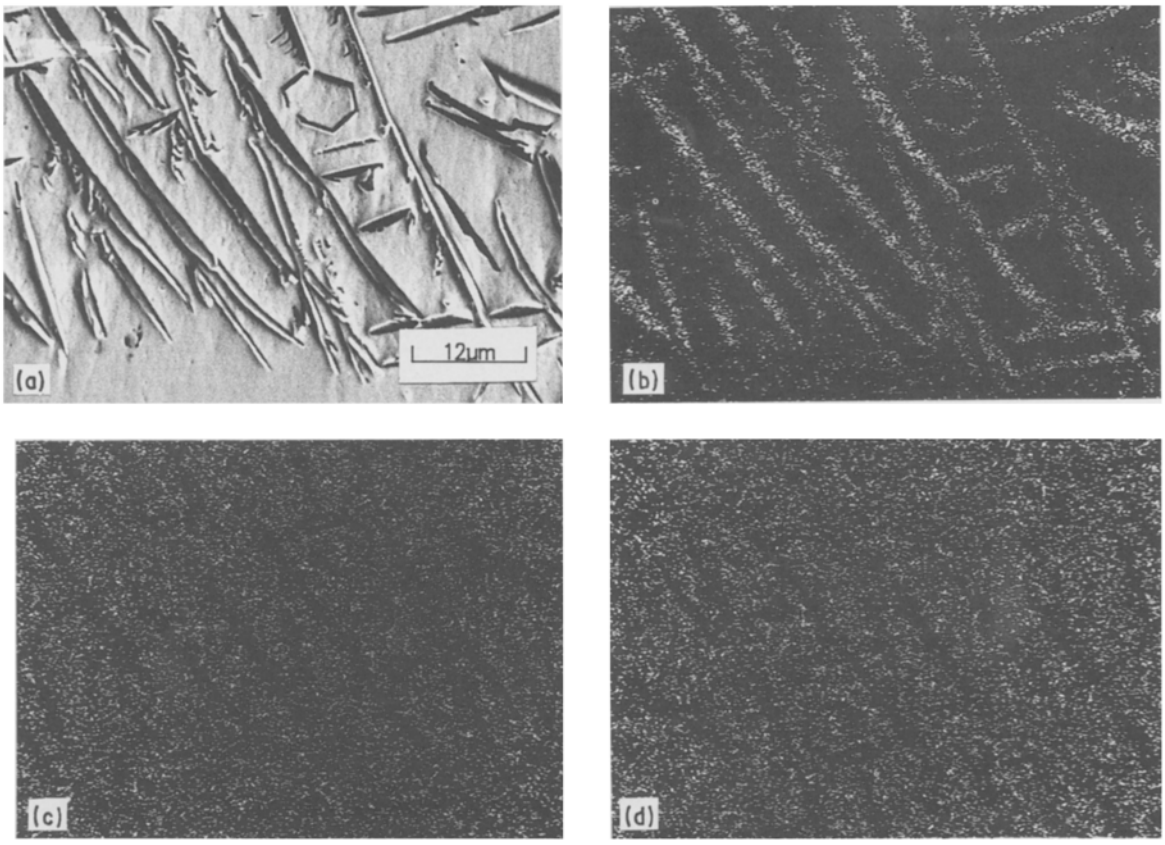

Figure 3 Scanning electron micrograph of the AlN on alloy E after 12 h in nitrogen at 1000° C. (a) Scanning electron micrograph, (b) X-ray map for aluminium, (c) X-ray map for manganese, (d) X-ray map for iron.

first diffuses into and becomes solute of the alloys and then reacts with aluminium. This is similar to or may even follow the same mechanism of internal oxide formation [12].

The internal oxidation process has been investigated by Rapp [13], Swisher [14] and Meijering [15]. In the same way, the depth of the layer containing AlN particles is the same as the zone of internal oxide, and should be equal to $(2D_N N_N t/N_{Al})^{1/2}$ which is derived by Wagner [12] where N_{Al} is the aluminium concentration in the matrix, N_N is the solubility of nitrogen in the alloy surface, D_N is the diffusivity of nitrogen in the alloy matrix. In the present work, the zone of internal nitride increases with increasing manganese concentration, which shows that increasing the manganese concentration will increase the permeability ($N_N D_N$) of nitrogen in the present Fe–Mn–Al–C alloy. Wang and Duh [7] studied the nitridation of Fe–31Mn–9Al–6Cr–0.87C alloy and suggested that the degree of solubility of nitrogen in the alloy plays the major role in AlN formation. This also indicates that such alloys must have a certain solubility and diffusivity for nitrogen which is sufficient to establish the required activity, N, of the dissolved nitrogen, along the AlN growth front.

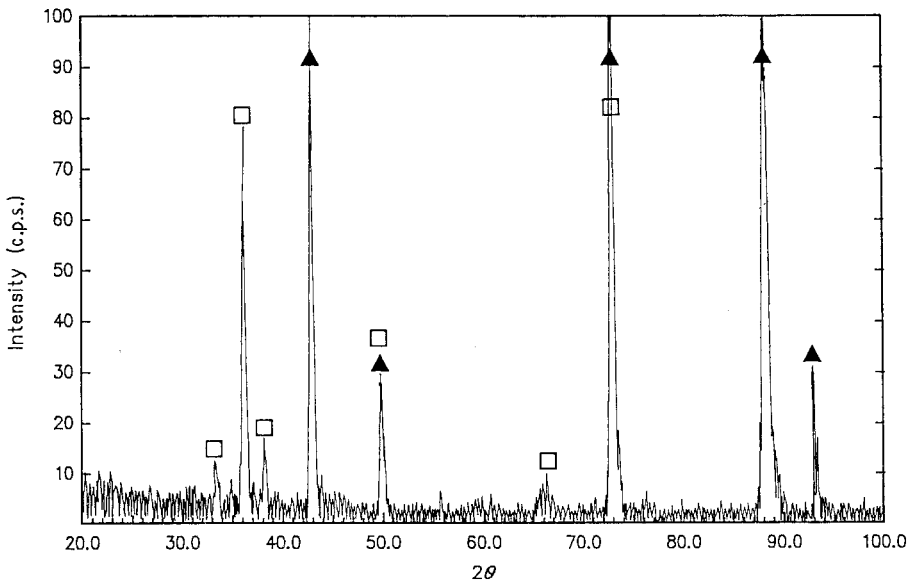

Figure 4 X-ray diffraction patterns of alloy E after 12 h in nitrogen at 1000° C. (□) AlN, (▲) γ.

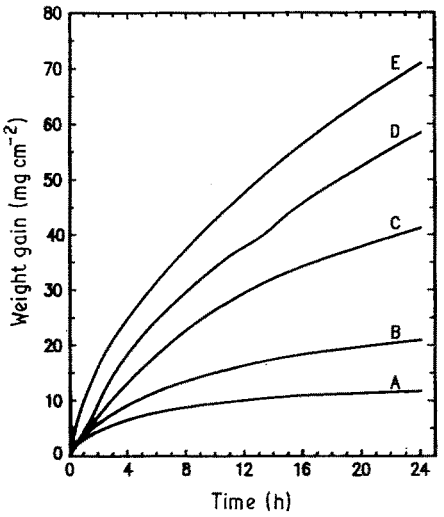

Figure 5 Thermogravimetric oxidation curve of the alloys used at 1000° C in air.

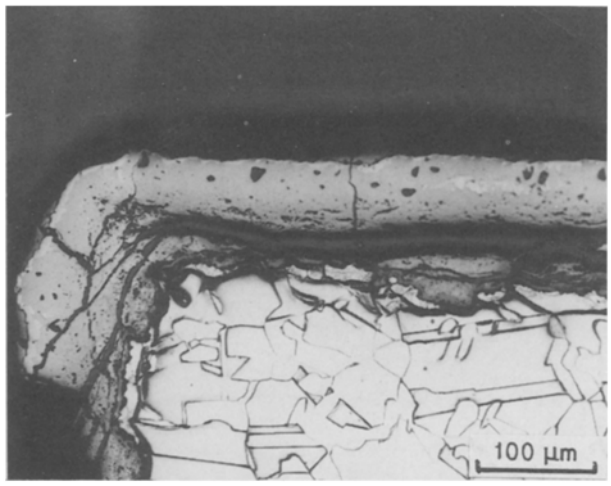

Figure 6 Metallographic cross-section of the oxide scale on alloy A after 6 h at 1000° C in air.

4.2. Behaviour in air

Because the high-temperature experiments at 1000° C are carried out in air which contains both nitrogen and oxygen, a close relationship between the formation of AlN and the manganese concentration in the alloys is always formed. The AlN particles are always observed underneath the oxide scale in alloys C, D and E which have high manganese contents of 31, 37 and 41 wt %, respectively. However, alloys A and B, which have lower manganese contents, have a lower permeability of nitrogen than alloys D and E, and no AlN particles are found after treatment at 1000° C in air. Here, (Fe, Mn)Al_2O_4 is always observed along the oxide/alloy interface.

The mechanism for the reaction of pure metal in a multicomponent gas at high temperature has been reviewed by Birks and Meier [16]. However, the reaction of a complicated alloy (Fe–Mn–Al–C) in a mixed gas (air) at high temperature is still unclear. Here, a tentative kinetics mechanism is proposed.

Based on thermodynamics, only aluminium can form a stable nitride in the present experiments at 1000° C. In addition, Al_2O_3 is more stable than AlN. In general, the initial stages of oxidation begin with the formation of nuclei of Al_2O_3, FeO, MnO, AlN, and CO (or CO_2), then AlN is rapidly displaced by Al_2O_3 and CO (or CO_2) evaporates into the environment. The oxidation rate of iron and manganese is

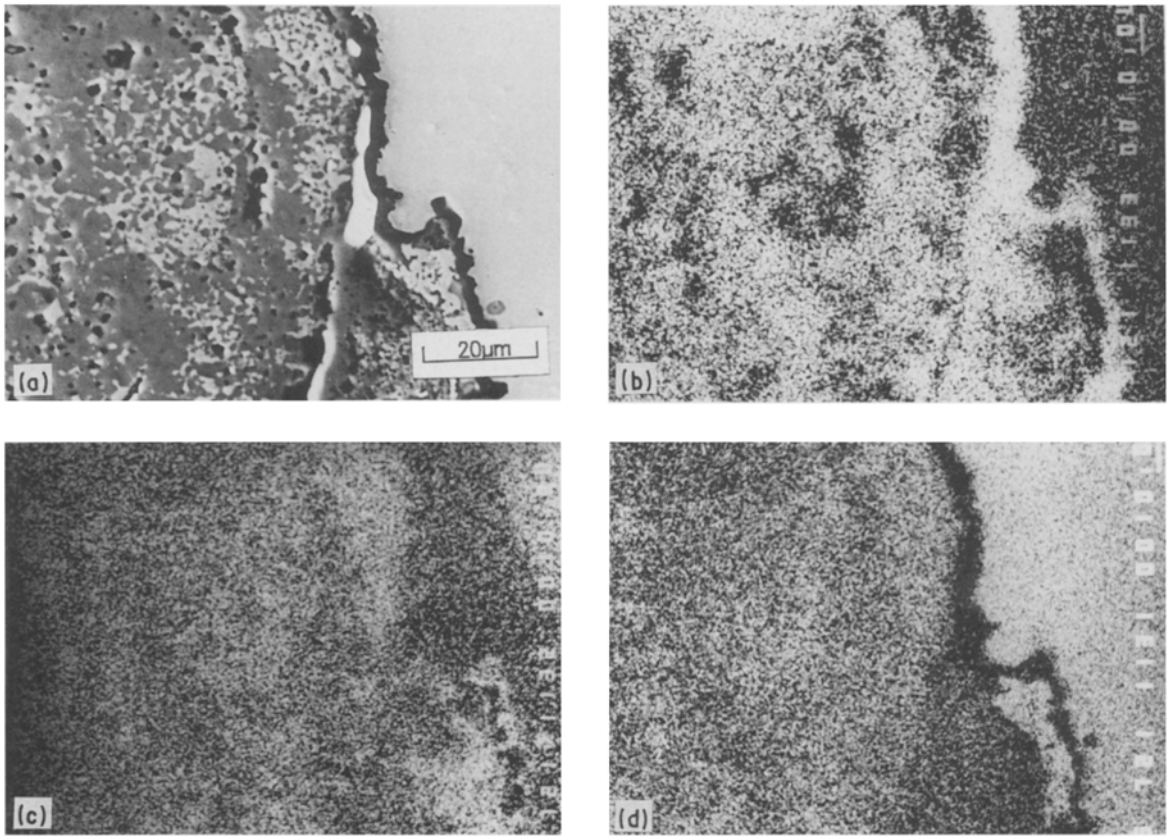

Figure 7 Scanning electron micrograph of the inner oxide layer of alloy A at 1000° C after 24 h in air. (a) Scanning electron micrograph, (b) X-ray map for aluminium, (c) X-ray map for manganese, (d) X-ray map for iron.

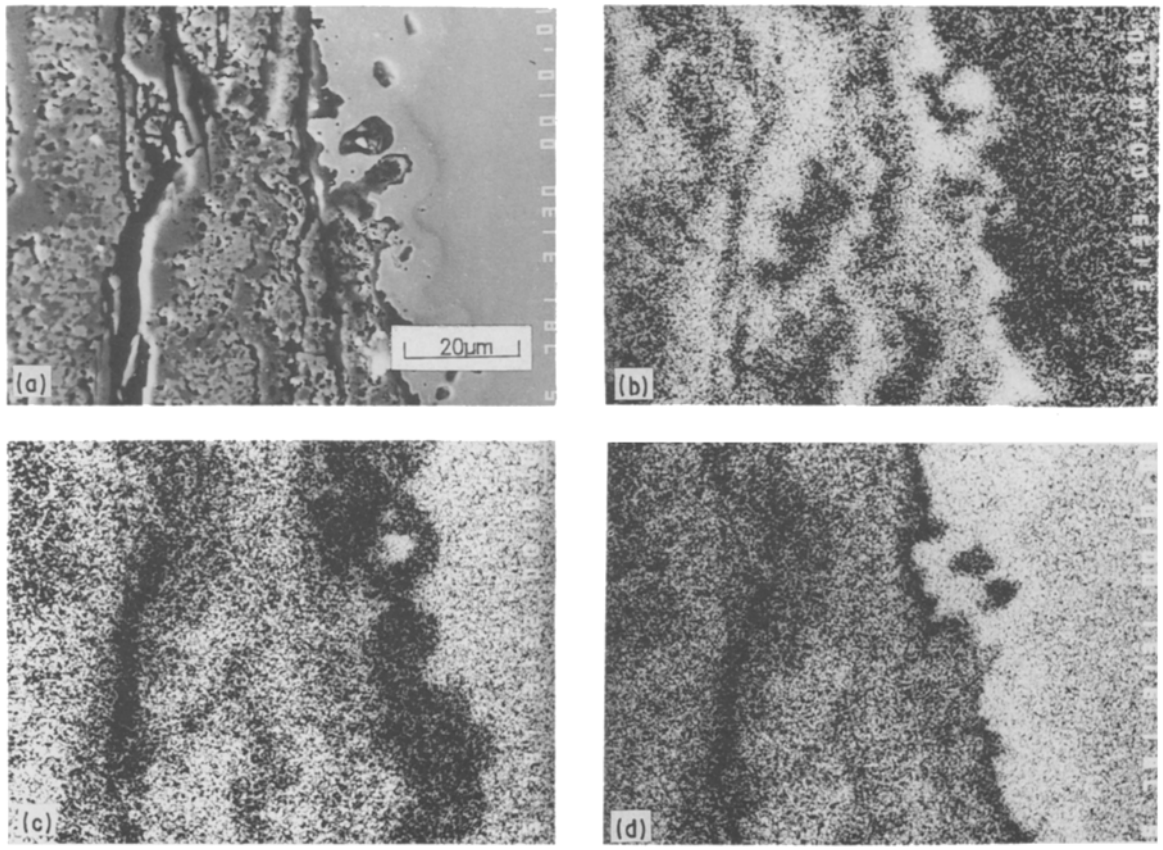

Figure 8 Scanning electron micrograph of the inner oxide layer of alloy B at 1000° C after 24 h in air. (a) Scanning electron micrograph, (b) X-ray map for aluminium, (c) X-ray map for manganese, (d) X-ray map for iron.

higher than that of aluminium [17] in the Fe–Mn–Al–C alloys. FeO and MnO always form rapidly on the alloy's surface and a continuous (Fe, Mn)O solid solution is primarily formed.

The dissociation pressure of MnO is about several orders of magnitude lower than FeO at 1000° C [17]. It is believed that more MnO is dissolved in (Fe, Mn)O and is accompanied by a lower dissociation pressure of (Fe, Mn)O. Based on gas kinetics theory, the effective collision rate of metal atoms and oxygen ($M + 1/2O_2 \rightarrow MO$) is proportional to $P_{O_2}^{1/2}$. It is reasonable to assume that the formation rate of MO is proportional to the effective collision rate, and the oxygen partial pressure in (Fe, Mn)O is equal to the equilibrium partial pressure of the oxides. In the present work, a clear approach is determined which indicates that more MnO is dissolved in (Fe, Mn)O in alloys C, D, E which have higher manganese concentrations. Thus, a lower formation rate of Al_2O_3 should be found along the (Fe, Mn)O/matrix interface.

In addition, the diffusion rate of aluminium in austenite is much lower than that in ferrite. Manganese is an austenite former and has the ability to lower the diffusion rate of carbon, thus it will depress the formation rate of the surface ferrite layer which is beneath the oxide scale. Therefore, it is difficult for aluminium to diffuse to the (Fe, Mn)O/matrix interface in those alloys which have higher manganese concentrations. According to Wagner [18], the protective external Al_2O_3 will form with difficulty.

In the present work, alloys C, D and E have a high permeability of nitrogen, thus nitrogen can penetrate easily through the less protective (Fe, Mn)O layer or the discontinuous $MnAl_2O_4$, and reacts with

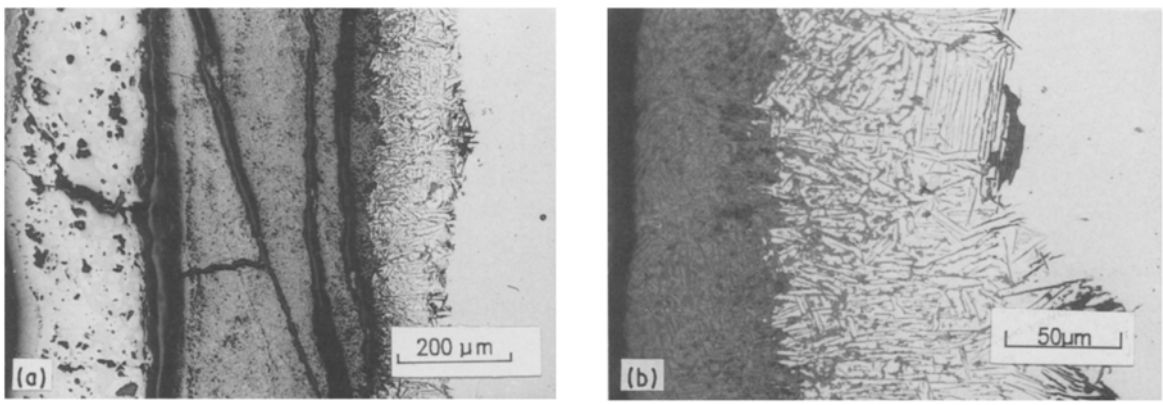

Figure 9 Alloy E after 6 h at 1000° C in air. (a) Metallographic cross-section of the oxide scale, (b) metallographic cross-section of the oxide/alloy interface.

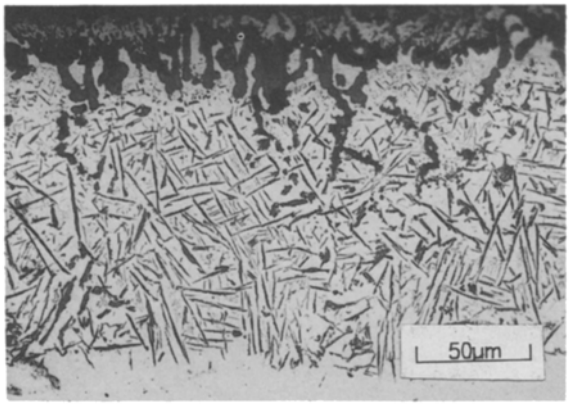

Figure 10 Metallographic cross-section of the scale/matrix interface of alloy E which was preoxidized in oxygen for 6 h then in nitrogen for 6 h at 1000° C.

aluminium to form AlN as shown in Fig. 10. For pure chromium which is oxidized in air [19], penetration of nitrogen through the Cr_2O_3 is also observed and the formation of Cr_2N is always promoted. These Cr_2N particles are also observed beneath the oxide scale. Therefore, the formation rate of Al_2O_3 is very low and the permeability of nitrogen is very high in alloys C, D, E which have comparable higher manganese concentrations in the present alloys. Thus, formation of AlN can be promoted and is located beneath the oxide scale for alloys C, D and E. Alloys A and B which have lower manganese concentrations, will have a higher Al_2O_3 formation rate. As the oxidation time increases, the formation of continuous (Fe, Mn)Al_2O_4 is suggested to occur through the chemical reaction between (Fe, Mn)O and Al_2O_3. (Fe, Mn)Al_2O_4 depresses the entry of nitrogen into the alloy [9]. Naturally, the formation of AlN is inhibited.

The mechanism by which manganese provides oxidation protection of Fe–Mn–Al steels seems to be analogous to that by which chromium affords protection to Fe–Mn–Al alloys [20], i.e. due to the dissociation oxygen pressure MnO existing between FeO and Al_2O_3. According to Wanger's secondary getter theory [20], the formation of FeO is suppressed and the formation of Al_2O_3 is promoted. For alloys C, D and E with manganese contents higher than 30 wt %, a continuous MnO layer is thought to be formed as the experiments are carried out in air at 1000° C. However, under such high manganese concentrations in alloys C, D and E, the formation rate of Al_2O_3 is lowered and AlN is formed beneath the oxide scale, as previously described. The needle-like AlN particles will consume the aluminium in alloy matrix and may provide an easy diffusion path for oxygen, nitrogen, iron and manganese. Thus, the appearance of such particles should render the oxidation resistance of Fe–Mn–Al–C alloys very poor.

5. Conclusions

1. Nitrogen is a second oxidant for alloys C, D and E in air at 1000° C in which the manganese content exceeds 30 wt %.

2. The addition of manganese would increase the permeability of nitrogen in Fe–Mn–Al–C alloys and is the main factor influencing the formation of AlN.

3. The formation of AlN is related to the low formation rate of Al_2O_3 and the high permeability of nitrogen in the alloys. Thus, AlN only can be formed in those alloys with higher manganese concentrations because the specimens are treated in air and in pure nitrogen at 1000° C.

Acknowledgement

The authors acknowledge the financial support of this research by National Science Council, Republic of China, under Grant NSC 76-0201-E007-12.

References

1. S. K. BANERJI, *Metal Progr.* **113** (4) (1978) 59.
2. C. J. LIN, Master Thesis, National Tsing Hua University, May 1982.
3. B. K. LEE, Master Thesis, National Tsing Hua University, May 1982.
4. J. P. SAUER, R. A. RAPP and J. P. HIRTH, *Oxid. Metal.* **18** (1982) 285.
5. P. R. S. JACKSON and G. R. WALLWORK, *ibid.* **21** (1984) 135.
6. M. F. S. LOPES and F. C. R. ASSUNCAO, "Alternate Alloying for environment Resistance", edited by G. R. Smolik and S. K. Banerji (The Metallurgical Society Inc., 1987).
7. C. J. WANG and J. G. DUH, *J. Mater. Sci.* **23** (1988) 2913.
8. C. H. KAO and C. M. WAN, *ibid.* **22** (1987) 3203.
9. T. MISHIMA and M. SUGIYAMA, *Tetsu to Hagnane* **36** (1950) 317.
10. P. MAYER and W. W. SMELTZER, *J. Electrochem. Soc.* **119** (1972) 626.
11. J. F. ELLIOT and M. GLEISER, "Thermochemistry for Steelmaking", Vol. 1, edited by Addison and Wesley (Massachussets, 1960).
12. C. WAGNER, *Z. Electrochem.* **63** (1959) 772.
13. R. A. RAPP, *Corrosion* **21** (1965) 382.
14. J. H. SWISHER, "Internal Oxidation" in "Oxidation of Metals and Alloys", edited by D. L. Douglass (ASM, Metals Park, Ohio, 1971) Ch. 12.
15. J. L. MEIJERING, "Internal Oxidation in Alloys", in "Advances in Materials Research", Vol. 5, edited by H. Herman (Wiley, New York, 1971) p. 1.
16. G. H. MEIER, Proceedings of Fourth Annual Conference on Materials for Coal Conversion and Utilization, NBS Gainthersburg, Maryland, October 1979, p. 164.
17. I. BARIN and O. KNACK, "Thermochemical Properties of Inorganic Substances" (Springer-Verlag, New York, 1973).
18. C. WAGNER, *Z. Electrochem.* **63** (1959) 772.
19. F. S. PETTIT, J. A. GOEBEL and G. W. GOWARD, *Corros. Sci.* **9** (1969) 903.
20. C. WAGNER, *ibid.* **5** (1965) 751.

Received 10 June
and accepted 7 December 1988